IOP Conf. Series: Journal of Physics: Conf. Series **783** (2017) 012028 doi:10.1088/1742-6596/783/1/012028

Improved LTVMPC design for steering control of autonomous vehicle

Shridhar Velhal

M.Tech Student, Department of Electrical Engineering, National Institute of Technology, Calicut, India

E-mail: shridharbvelhal@gmail.com

Susy Thomas

Professor, Department of Electrical Engineering, National Institute of Technology, Calicut, India

E-mail: susy@nitc.ac.in

Abstract. An improved linear time varying model predictive control for steering control of autonomous vehicle running on slippery road is presented. Control strategy is designed such that the vehicle will follow the predefined trajectory with highest possible entry speed. In linear time varying model predictive control, nonlinear vehicle model is successively linearized at each sampling instant. This linear time varying model is used to design MPC which will predict the future horizon. By incorporating predicted input horizon in each successive linearization the effectiveness of controller has been improved. The tracking performance using steering with front wheel and braking at four wheels are presented to illustrate the effectiveness of the proposed method.

1. Introduction

In this paper, the problem being addressed is the steering control of autonomous vehicle for effective tracking of predefined trajectory. A double lane change scenario on slippery road is considered as trajectory. The assumption is that a trajectory planning system is available for designing the path to be followed. The problem involves yaw and lateral vehicle dynamics stabilization via steering control while tracking a desired path as close as possible while fulfilling the physical constraints. In [1][2][3][4] this problem has been addressed using front wheel steering control where the authors rely on linear time varying model predictive control (LTVMPC) for the controller design. In [4] the authors have improved the design by incorporating braking at four wheels to the steering control. In the work reported in this paper this design is further improved by modifying the linearization process involved in controller design.

Model predictive control (MPC) qualifies to be an adequate control strategy by virtue of its capacity to predict the future states and to handle constraints. In MPC a model of the plant is used to predict the future horizon of states of system. Based on this prediction horizon at each sampling time t, a performance index is optimized under operating constraints. Optimization gives sequence of future input moves in order to best follow a given trajectory. The first of

the optimal moves is the control action applied to the plant at time t. At time t+1, a new optimization is defined and solved over a shifted prediction horizon [5] [6].

The nonlinear vehicle model discussed in [1] is being considered for the LTVMPC design. For nonlinear model, predictions of horizon based on nonlinear equations are very complex involving difficult computation. For such systems a sub-optimal controller using successive linearization is often used. In [1][2][3] the authors depend on such a methodology for controller design using front wheel steering.

The reported LTVMPC [3], uses a linearized state space model to predict the future horizon. For a time t, predictions are calculated using linearized model obtained by successive linearization at each sampling instant. This model is then used for the calculation of next input horizon. In next sampling instant this procedure of modeling and computing control horizon is repeated. In the methodology used in [3], at every instant successive linearization makes use of the previous input. Since predicted input is available at every instant, the accuracy of linearization process can be improved by making use of this predicted value rather than previous input as this will reduce the approximation involved in jacobian matrix of linearized model. This improvisation in successive linearization of system leads to better tracking performance compared to the methodology in [3]. This has been verified by applying this proposed method to the same autonomous vehicle being used in [3] [4]

The control inputs being used are front steering angle and braking at each wheel. Steering angle and its rate of change has physical limitations which has been taken into consideration in design. Also brakes are being applied within limits so that stability is maintained.

The paper is structured as follows: Section II describes the system model which includes vehicle model and tyre model in detail. Since the proposed improved LTVMPC method relies on LTVMPC methodology reported in [3], section III describes this methodology first and then deals with the proposed method. Simulation results are presented in section IV to illustrate the effectiveness of this method. Section V concludes the paper.

2. System model

The vehicle dynamic model as given in [1][2][3][4] is presented in this section. Fig 1 shows schematic of four wheel autonomous vehicle.

The two front and two rear wheels of car are denoted by $\star \in \{f, r\}$ and the left and right wheels by $\bullet \in \{l, r\}$. $F_{l\star,\bullet}$, $F_{c\star,\bullet}$ denotes longitudinal and lateral tire forces receptively. $F_{x\star,\bullet}$, $F_{y\star,\bullet}$ are forces in car body frame, F_z is normal tire load. I denotes the inertia of car, a, b are distance of front and rear wheels from center of gravity of car, c is the distance of vehicle longitudinal axis from wheels, g is gravitational constant, m is car mass, r is wheel radius, ψ is heading angle, X, Y are absolute car position coordinates (global reference), $s_{\star,\bullet}$ are slip ratios for four wheels, $\dot{x}$ is the longitudinal speed of vehicle, $\dot{y}$ is the lateral speed of vehicle, $\alpha_{\star,\bullet}$ are slip angles at four wheels, $\delta_{\star,\bullet}$ are wheel steering angle at each wheel and $\mu_{\star,\bullet}$ is road friction coefficient at the four wheels.

2.1. Vehicle model

Assuming the mass of vehicle to be constant, the normal tyre force (i.e. vertical force on tire) F_z is constant, the dynamics of four wheel model as shown in fig 1 is represented by following equations :

$$m\ddot{x} = m\dot{y}\dot{\psi} + F_{x_{f,l}} + F_{x_{f,r}} + F_{x_{r,l}} + F_{x_{r,r}} \tag{1a}$$

$$m\ddot{y} = -m\dot{x}\dot{\psi} + F_{y_{f,l}} + F_{y_{f,r}} + F_{y_{r,l}} + F_{y_{r,r}} \tag{1b}$$

$$\begin{aligned} I\ddot{\psi} &= a(F_{y_{f,l}} + F_{y_{f,r}}) - b(F_{y_{r,l}} + F_{y_{r,r}}) \\ &\quad +c(-F_{x_{f,l}} + F_{x_{f,r}} - F_{x_{r,l}} + F_{x_{r,r}}) \end{aligned} \tag{1c}$$

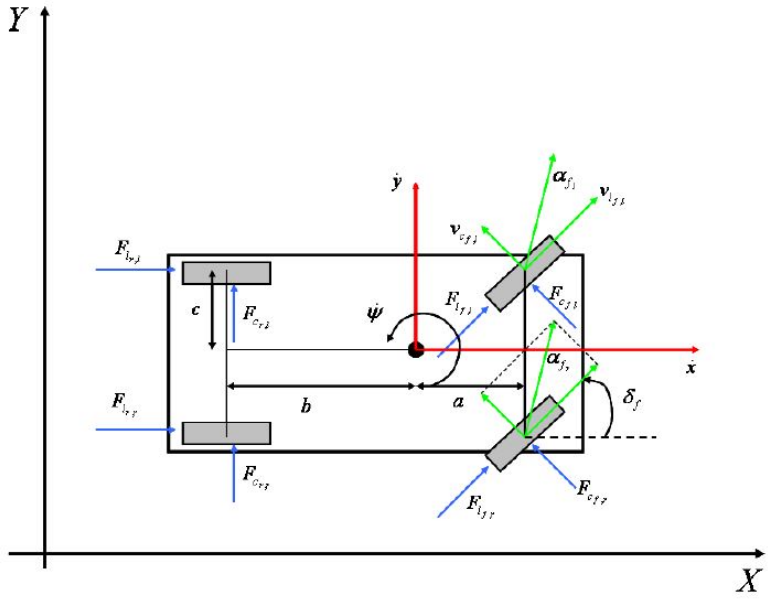

Figure 1: Vehicle model

The equations of motion in an absolute inertial frame are :

$$\dot{X} = \dot{x}\cos\psi - \dot{y}\sin\psi \tag{2a}$$
$$\dot{Y} = \dot{x}\sin\psi + \dot{y}\cos\psi \tag{2b}$$

Longitudinal and lateral tire forces lead to the following forces acting on the center of gravity :

$$F_{y_{\star,\bullet}} = F_{l_{\star,\bullet}}\sin\delta_{\star,\bullet} + F_{c_{\star,\bullet}}\cos\delta_{\star,\bullet} \tag{3a}$$
$$F_{x_{\star,\bullet}} = F_{l_{\star,\bullet}}\cos\delta_{\star,\bullet} - F_{c_{\star,\bullet}}\sin\delta_{\star,\bullet} \tag{3b}$$

Tire forces for each tire are given by [7] :

$$F_{l_{\star,\bullet}} = f_l(\alpha_{\star,\bullet}, s_{\star,\bullet}, \mu_{\star,\bullet}, F_z) \tag{4a}$$
$$F_{c_{\star,\bullet}} = f_c(\alpha_{\star,\bullet}, s_{\star,\bullet}, \mu_{\star,\bullet}, F_z) \tag{4b}$$

The tire slip angle represents the angle between the wheel velocity and the direction of the wheel itself and can be expressed as :

$$\alpha_{\star,\bullet} = \tan^{-1}\frac{v_{c_{\star,\bullet}}}{v_{l_{\star,\bullet}}} \tag{5}$$

The slip ratio formula is defined as :

$$s = \frac{r\omega}{v_l} - 1, \qquad if\ v_l > r\omega,\ v \neq 0 \qquad for\ braking \tag{6a}$$
$$s = 1 - \frac{v_l}{r\omega}, \qquad if\ v_l < r\omega,\ \omega \neq 0 \qquad for\ driving \tag{6b}$$

The lateral (or cornering) and longitudinal wheel velocities are :

$$v_{l_{\star,\bullet}} = v_{y_{\star,\bullet}}\sin\delta_{\star,\bullet} + v_{x_{\star,\bullet}}\cos\delta_{\star,\bullet} \tag{7a}$$
$$v_{c_{\star,\bullet}} = v_{y_{\star,\bullet}}\cos\delta_{\star,\bullet} - v_{x_{\star,\bullet}}\sin\delta_{\star,\bullet} \tag{7b}$$

and

$$v_{y_{f,l}} = \dot{y} + a\dot{\psi} \qquad v_{x_{f,l}} = \dot{x} - c\dot{\psi} \tag{8a}$$
$$v_{y_{f,r}} = \dot{y} + a\dot{\psi} \qquad v_{x_{f,l}} = \dot{x} + c\dot{\psi} \tag{8b}$$
$$v_{y_{r,l}} = \dot{y} - b\dot{\psi} \qquad v_{x_{f,l}} = \dot{x} - c\dot{\psi} \tag{8c}$$
$$v_{y_{r,r}} = \dot{y} - b\dot{\psi} \qquad v_{x_{f,l}} = \dot{x} + c\dot{\psi} \tag{8d}$$

The parameter $\mu_{\star,\bullet}$ denotes the road frictional coefficients and are assumed equal for all the four wheels. F_z is the total vertical load of the vehicle and is distributed between the front and rear wheels based on the geometry of the car model (described by the parameters a and b) is given by :

$$F_{z_f} = \frac{\text{bmg}}{2(a+b)}, \qquad F_{z_r} = \frac{\text{amg}}{2(a+b)} \tag{9}$$

Equations (1)-(9) describes the nonlinear vehicle dynamics. For simplicity of representation this is expressed as :

$$\frac{d\xi}{dt} = f_{s(t),\mu(t)}(\xi(t), u(t)) \tag{10}$$

The state and input vectors are given by,

$$\xi = [\dot{y} \quad \dot{x} \quad \psi \quad \dot{\psi} \quad Y \quad X]^T \tag{11}$$
$$u = [\delta_{fl} \quad \delta_{fr} \quad \delta_{rl} \quad \delta_{rr} \quad s_{fl} \quad s_{fr} \quad s_{rl} \quad s_{rr}]^T \tag{12}$$

The front wheel steering model is obtained by letting $\delta_{fl} = \delta_{fr} = \delta_f$ and $\delta_{rl} = \delta_{rr} = \delta_r = 0$.

2.2. Tyre model

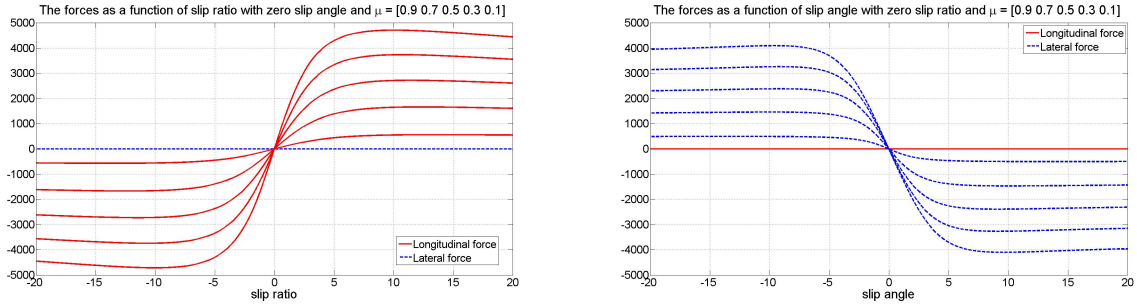

(a) longitudinal force (b) lateral force

Figure 2: Longitudinal and lateral tire forces with different frictional coefficient (μ) values. [7]

The model for tyre tractive and cornering forces presented in [3] are based on magic formula described by Pacejka model [7]. The same tyre model has been used in this paper.

The Pacejka tire model calculates lateral force and longitudinal force based on percent longitudinal slip (slip ratio), slip angle, frictional coefficient and vertical normal force. Figure 2 shows the longitudinal and lateral forces versus slip ratio and slip angle respectively for constant friction coefficient and vertical load.

3. Controller design

In MPC at each sampling time, an optimal control problem is solved over a finite horizon. The optimal control problem minimizes the performance index, subject to operating constraints. The resulting optimal command signal is applied to the vehicle system for that sampling interval. At the next instant, a new optimal control problem is solved for new measurements of the state over the shifted horizon. MPC is a step by step procedure where design ensures that states and control input are satisfying their constraints. As the problem being considered is steering control with braking and all outputs are to be tracked output constraints does not figure in problem. The continuous time model given in eq (10) is discretized with T_s as sampling time. This discretized model is represented by :

$$\begin{aligned} \xi(k+1) &= f_{s(k),\mu(k)}(\xi(k), \Delta u(k)) && (13) \\ u(k) &= u(k-1) + \Delta u(k) && (14) \end{aligned}$$

3.1. LTV model

Controller design for nonlinear systems are made simple by linearizing the system model around its operating point. By successive linearization over each shifting operating point the accuracy of the MPC design for autonomous vehicle can be improved. Such a model is referred to as linear time varying (LTV) model.

With the initial state $\xi_0 \in X$ and initial control input $u_0 \in U$, the one step ahead dynamics of system is :

$$\begin{aligned} \xi(k+1) &= f(k, \hat{\xi}_0(k), \Delta u(k)) && (15) \\ u(0) &= u_0 \\ \hat{\xi}(0) &= \xi_0 \end{aligned}$$

Linearization of eq (13) about its initial condition will lead to :

$$\xi(k+1) = A_{k,0}\xi(k) + B_{k,0}u(k) + Bw_{k,0}W(k) \quad (16)$$

where,

$$\begin{aligned} A_{k,0} &= \left.\frac{\partial f}{\partial \xi}\right|_{\hat{\xi}_0(k),u_0} && (17a) \\ B_{k,0} &= \left.\frac{\partial f}{\partial u}\right|_{\hat{\xi}_0(k),u_0} && (17b) \\ \delta\xi(k) &= \xi(k) - \hat{\xi}_0(k) && (17c) \end{aligned}$$

Bw is the input matrix for disturbance and $W(k)$ is the disturbance to system.

3.2. LTVMPC controller

The MPC designed for linear model in eq (16) is referred to as LTVMPC [1] [2] [3] [4]. The fact that, the model in eq (16) is recalculated at every sampling instant justifies the term LTV. At each sampling instant t, the system dynamics can be represented as :

$$\xi(k+1) = A_{k,t}\xi(k) + B_{k,t}u(k) + Bw_{k,0}W(k) \quad (18)$$

The matrices $A_{k,t}, B_{k,t}$ are as defined in eq (17), where fixed initial index of zero is replaced by current time t.

$$A_{k,t} = \left.\frac{\partial f}{\partial \xi}\right|_{\hat{\xi}(k,t),u_t} \qquad B_{k,t} = \left.\frac{\partial f}{\partial u}\right|_{\hat{\xi}(k,t),u_t} \quad (19)$$

and,

$$\begin{aligned} \hat{\xi}(k+1,t) &= f(\hat{\xi}(k,t),\Delta u_t,t), \quad k=t,t+1,...t+N-1 && \text{(20a)} \\ \hat{\xi}(t,t) &= \xi_t && \text{(20b)} \\ u_t &= u_{t-1} && \text{(20c)} \end{aligned}$$

For the above system, control horizon is generated by minimizing cost function J_N given by :

$$\begin{aligned} J_N(\xi_t,\Delta U_t,\Xi_{reft}) &= \sum_{i=1}^{n_y}\|(\eta_{t+i,t}-\eta ref_{t+i,t})\|_Q^2+\sum_{i=0}^{n_u-1}\|\Delta u_{t+i,t}\|_R^2 \\ &\quad +\sum_{i=0}^{n_u-1}\|u_{t+i,t}\|_\lambda^2+\rho\epsilon \end{aligned} \tag{21}$$

where $\eta = [\ \ velocity\ \ \dot{\psi}\ \ \psi\ \ Y\ \ ]$ are the output variables of the system and ηref denote the corresponding reference signal. n_u is size of input prediction horizon and n_y is size of output prediction horizon. $\Delta U_t = [\ \ \Delta u_t\ \ \Delta u_{t+1}\ \ .\ \ .\ \ \Delta u_{t+n_u-1}\ \ ]$ *and* $\Xi_{ref}(t) = [\eta_{ref}(t+1)\ \ \eta_{ref}(t+2)\ \ .\ \ \eta_{ref}(t+n_y)]$ are the sequence of input and reference trajectory over time horizon n_u and n_y respectively.

Eq (21) indicates that the cost function involves trajectory tracking with weight Q while minimizing both control effort and its increment with weights λ and R respectively.

At each sampling instant t, the cost function given in eq (21) is minimized. The optimization problem can be stated as follows :

$$\min_{\Delta U_t}\ J(\xi_t,\Delta U_t,\Xi_{ref_t})$$

$$\begin{aligned} \text{s.t.}\quad \xi_{k+1,t} &= A_{k,t}\xi_{k,t}+B_{k,t}u_{k,t}+d_{k,t} \\ \alpha_{k,t} &= \mathcal{C}_t\xi_{k,t}+\mathcal{D}_t u_{k,t} \\ \Delta u_{\min} &\le \Delta u_{k,t} \le \Delta u_{\max} \\ u_{\min} &\le u_{k,t} \le u_{\max} \\ u_{k,t} &= u_{k-1,t}+\Delta u_{k,t} \\ \alpha_{\min}-\epsilon &\le \alpha_{k,t} \le \alpha_{\max}+\epsilon \end{aligned} \tag{22}$$

In eq (22) α is the slip angle which is the constrained output. The constraint on α is soft constraint defined using slack variable ε [9] [10]. The soft constraint are those which can be violated. However the weight factor on the violation ensures that violation penalizes the cost function as indicated by the term $\rho\xi$ in eq (21).

The optimization problem stated in eq (22) can be reformulated as a quadratic problem (QP). The details of quadratic programming and MPC control law has been discussed in [5]-[6]. The sequence of optimal input deviations are computed at every sampling time t by solving (22). The optimal control horizon is

$$\Delta U^*_{t,t} = [\ \ \Delta u^*_{t,t}\ \ \Delta u^*_{t+1,t}\ \ .\ \ .\ \ .\ \ \Delta u^*_{t+n_u-1,t}\ \ ] \tag{23}$$

Only the first deviation value is used to obtain optimal control at instant t

$$\begin{aligned} u_t &= u_{t-1}+\Delta u^*_{t,t} && \text{(24)} \\ \hat{u}_{t+1} &= u_t+\Delta u^*_{t+1,t} && \text{(25)} \end{aligned}$$

As already explained, at each sampling time t, the linear model is computed by linearization of (13) around state ξ_t and input u_t.

In [1][3][4] for linearization the input used is $u_t = u_{t-1}$ as indicated by (20c), which is not correct in the strict sense. Since MPC is capable of generating the predicted input at instant t which is a better approximation to the actual u_t than u_{t-1}, the linearized model with predicted $\hat{u}_t$ will reduce the error involved in the approximation. For incorporating this improvement, u_{t-1} in (20c) is replaced by $\hat{u}_t$ computed as follows:

$$\hat{u}_t = u_{t-1} + \Delta u^*_{t,t-1} \tag{26}$$

As ideal MPC control law always follows the tail of previous input horizon, the above predicted control is a logical improvisation to equating u_t to u_{t-1}.

In LTV model, over a prediction horizon state space model is assumed to be constant. At next sampling instant $(t+1)$, the horizon moves one step and the system is linearized and optimization problem defined by eq (22) is solved based on the state ξ_{t+1} and input $\hat{u}_{t+1}$.

Use of eq (20c) rather than eq (26) in each successive linearization steps is bound to add to the tracking error because of the cumulative effect of the approximation error.

The improvised model which makes use of eq (26) is seen to fetch better tracking. This is presented in simulation results.

4. Simulation results

As in [1][2][3][4], it is assumed that vehicle is entering a double lane change maneuver on very low frictional road with a given initial speed. The control input is the steering angle and the goal is to follow the trajectory as close as possible by minimizing the vehicle deviation from the target path with highest possible entry speed. In [1][2] only steering control has been used for trajectory tracking. In [3][4] both steering and braking control has been used for this purpose. The simulation results presented in this section are based on both steering and braking. As in [4] a vehicle speed of $21m/sec$ is considered for simulation. As in [1][2][3][4] The reference model for MPC used is same as the system model at starting point. The simulation results for the improved LTVMPC are in accordance with the expected improvement in tracking error.

The control inputs are the front wheel steering angle and slip ratios at the four wheels. Following has been used for tuning of controller :

- Sample time T = 0.05 sec.
- Constraints on steering input and input increments : $\delta_{fmin} = -10°, \delta_{fmax} = 10°, \Delta\delta_{fmin} = -0.85°, \Delta\delta_{fmax} = 0.85°$
- The upper and lower bounds on four slip ratio are 0% and -2.7% respectively. The upper and lower bounds on braking rate are 10 % and -10% respectively.
- Weights on tracking errors: $Q_{\dot{x}} = 0.5, Q_{\psi} = 12000, Q_{\dot{\psi}} = 3000, Q_Y = 600$
- Weights on input rates: $R_{\delta_f} = 5000, R_{s_{\star,\bullet}} = 50$
- Weights on inputs: $\lambda_{\delta_f} = 1000, \lambda_{s_{\star,\bullet}} = 16$
- Horizon $n_y = 21, n_u = 10$
- Constraints on the tyre slip angles: $\alpha_{min} = -3°, \alpha_{max} = 3°$
- Weight on soft constraint $\rho = 28$
- Entry velocity of vehicle $v = 21m/sec$
- Road friction $\mu_{\star,\bullet} = 0.3$

In figures 3 - 5 simulation results obtained by using the LTVMPC design as reported in [4] are shown. The entry speed of $21m/sec$ is reduced to $18.75m/sec$ at the end of double lane change as seen in fig 3(a). The tracking performance with LTVMPC for ψ, Y, $\dot{\psi}$ are shown in fig 3(b), 3(c), 3(d) respectively.

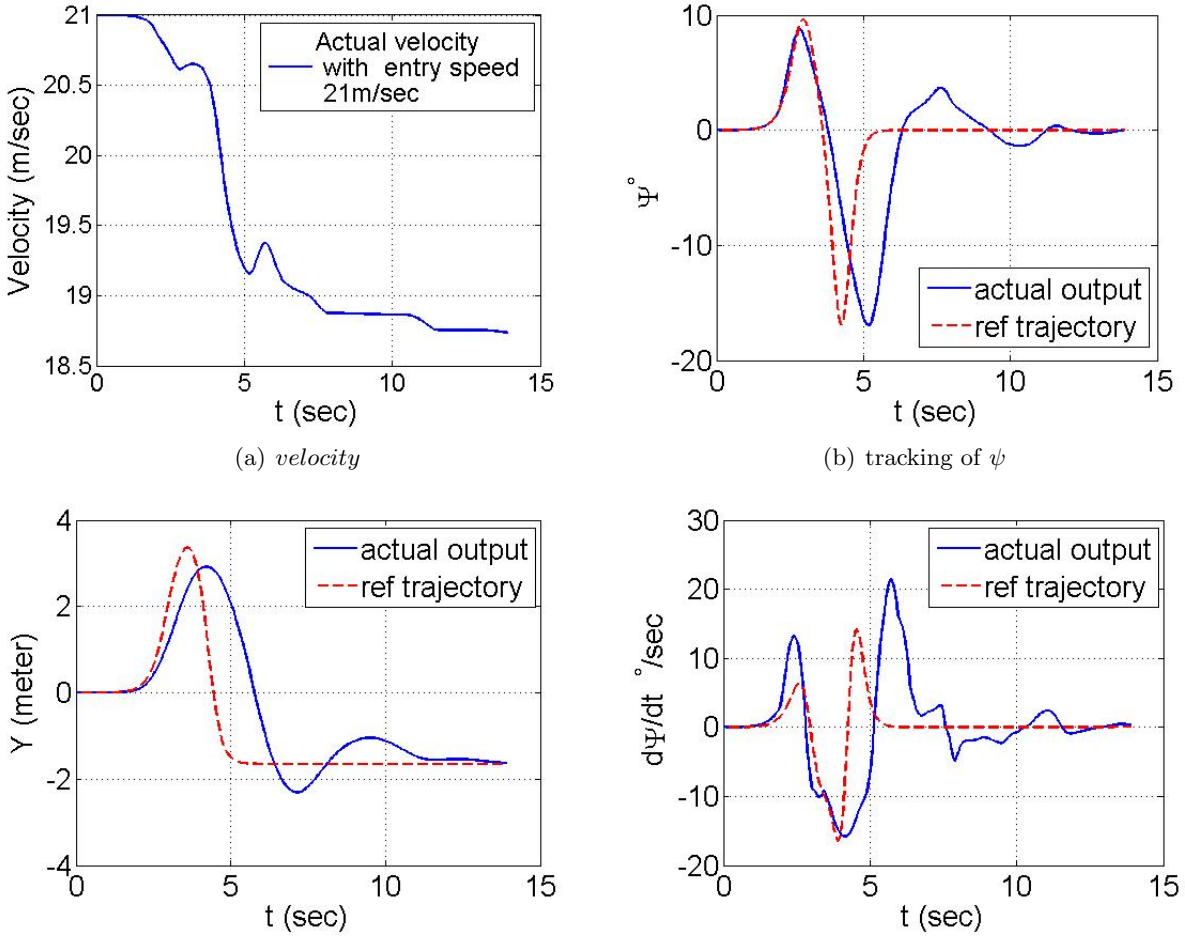

(a) *velocity* (b) tracking of ψ

(c) tracking of Y (d) tracking of $\dot{\psi}$

Figure 3: Tracking with LTVMPC.

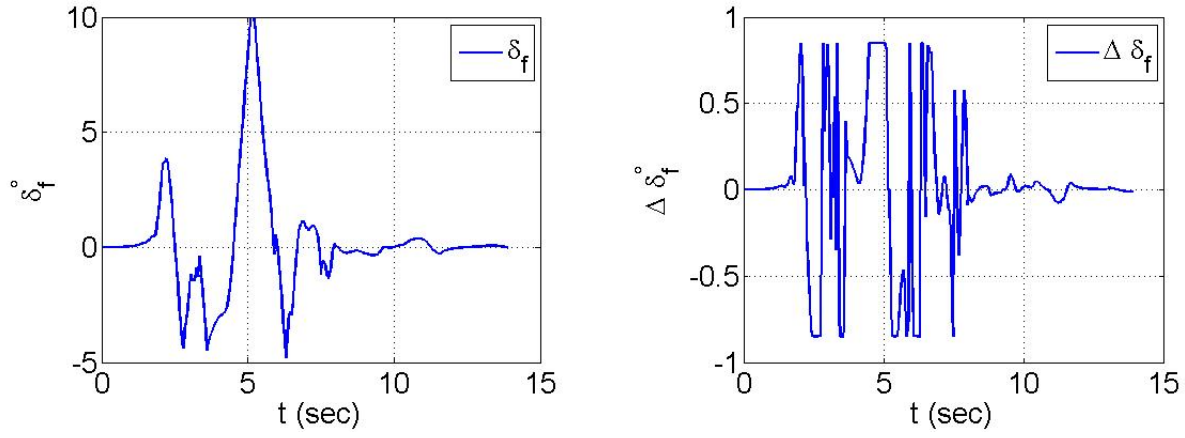

(a) input δ_f (b) input $\Delta\delta_f$

Figure 4: Input and input increment of front wheel steering angle with LTVMPC.

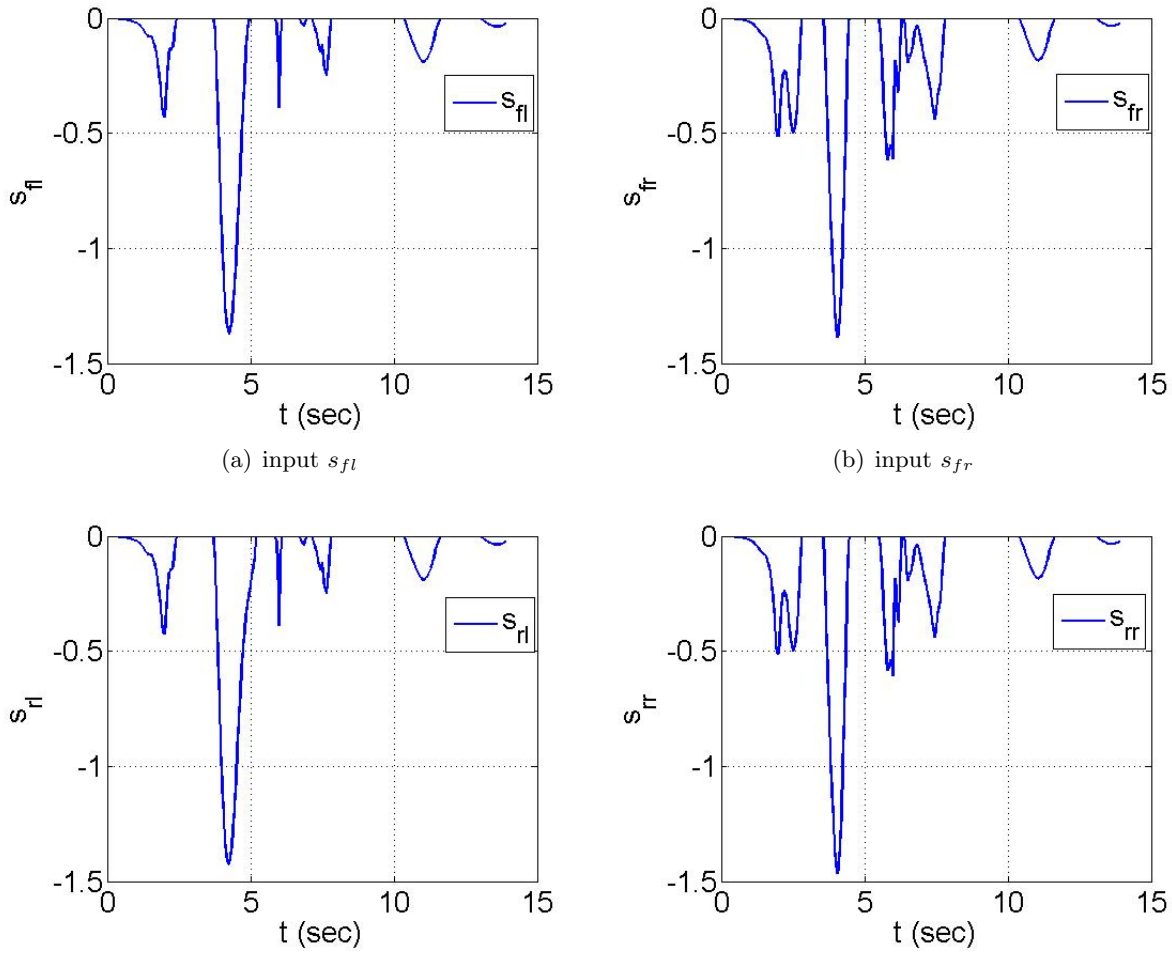

(a) input s_{fl} (b) input s_{fr}

(c) input s_{rl} (d) input s_{rr}

Figure 5: Slip ratios at four wheels with LTVMPC.

Fig 4 shows the steering angle and increments of steering angle for LTVMPC. Both these values are bounded within the constraints.

Fig 5 shows the slip ratio at the four wheels for LTVMPC. It can be seen that the slip ratio of right side front and rear wheels are similar to each other. Also for left side front and rear slip ratio are similar. More braking is applied to right side wheels. This input provides differential braking which helps to turn right. This shows that braking is not only applied to reduce speed of vehicle but also to help the steering.

In figures 6 - 8 simulation results of the proposed improved LTVMPC controller are shown. The entry speed of $21m/sec$ is reduced to $19.10m/sec$ which is an improvisation on the achieved speed of $18.75m/sec$ with LTVMPC. Comparison of the velocity profile in fig 3(a) and fig 6(a) shows an improvement in velocity profile for the proposed method towards the latter half of lane change where it is seen that velocity profile continuously maintains a higher velocity than the velocity observed in fig 3(a).

The tracking performance with improved LTVMPC for ψ, Y, $\dot{\psi}$ are shown in fig 6(b), 6(c), 6(d) respectively. An improvement in tracking of Y for improved LTVMPC can be seen in fig

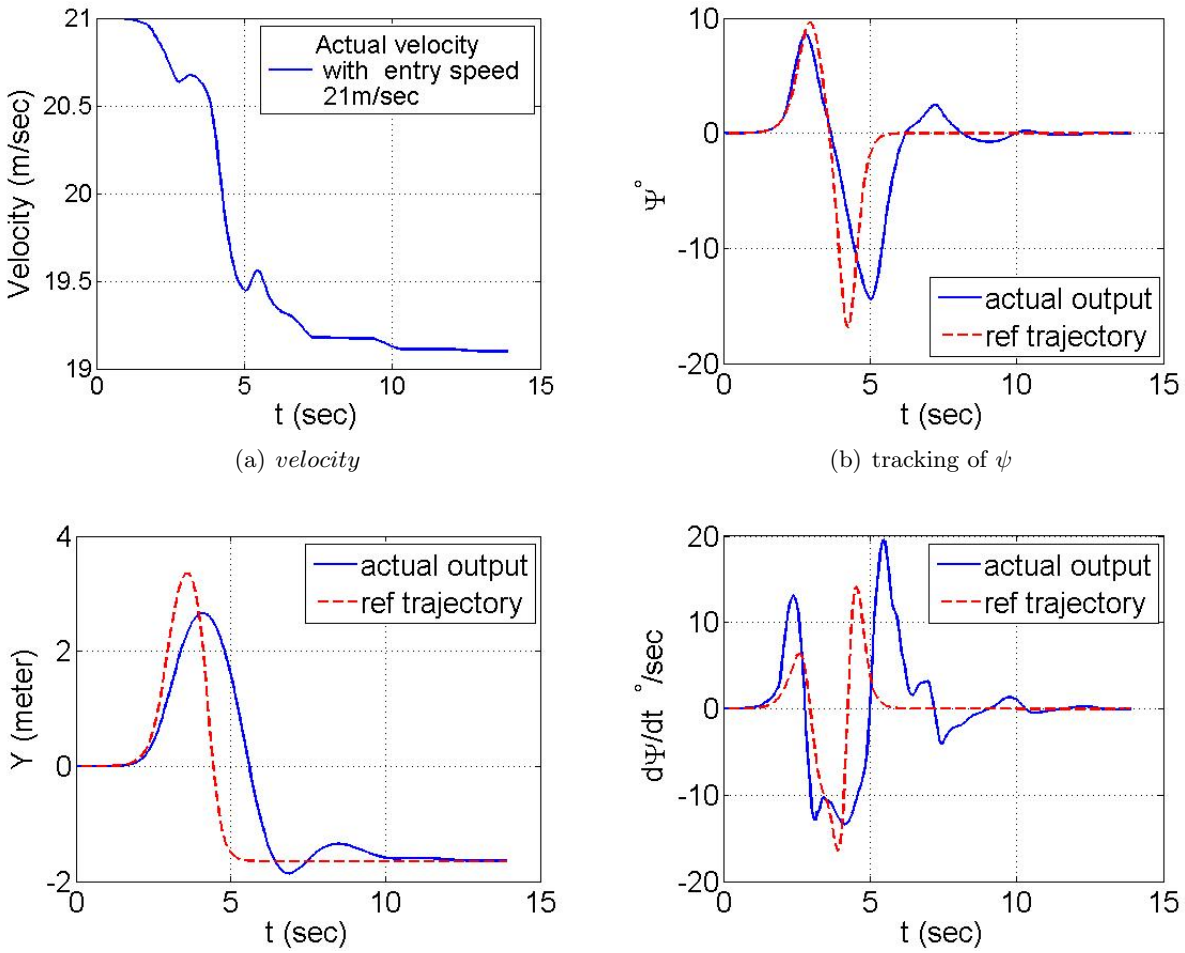

(a) *velocity* (b) tracking of ψ

(c) tracking of Y (d) tracking of $\dot{\psi}$

Figure 6: Tracking with improved LTVMPC.

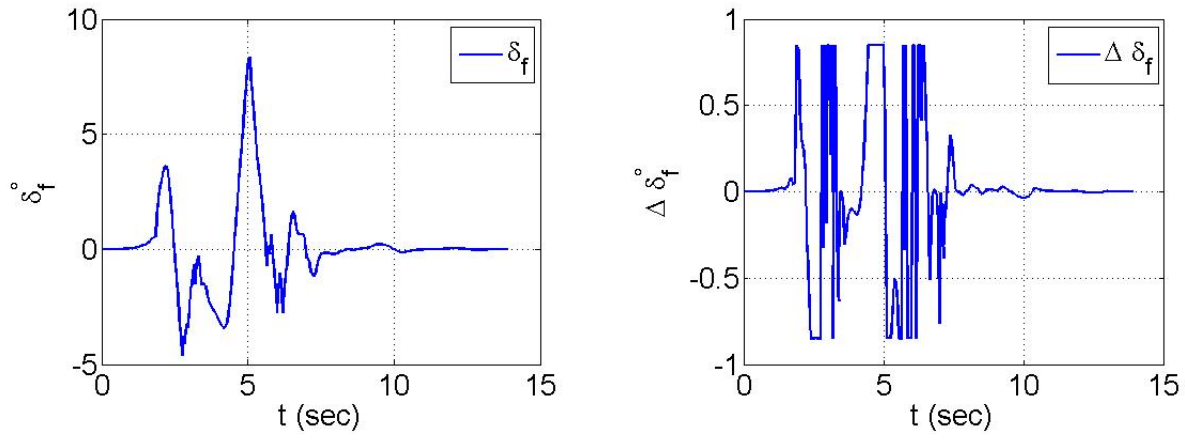

(a) input δ_f (b) input $\Delta\delta_f$

Figure 7: Input and input increment of front wheel steering angle with improved LTVMPC.

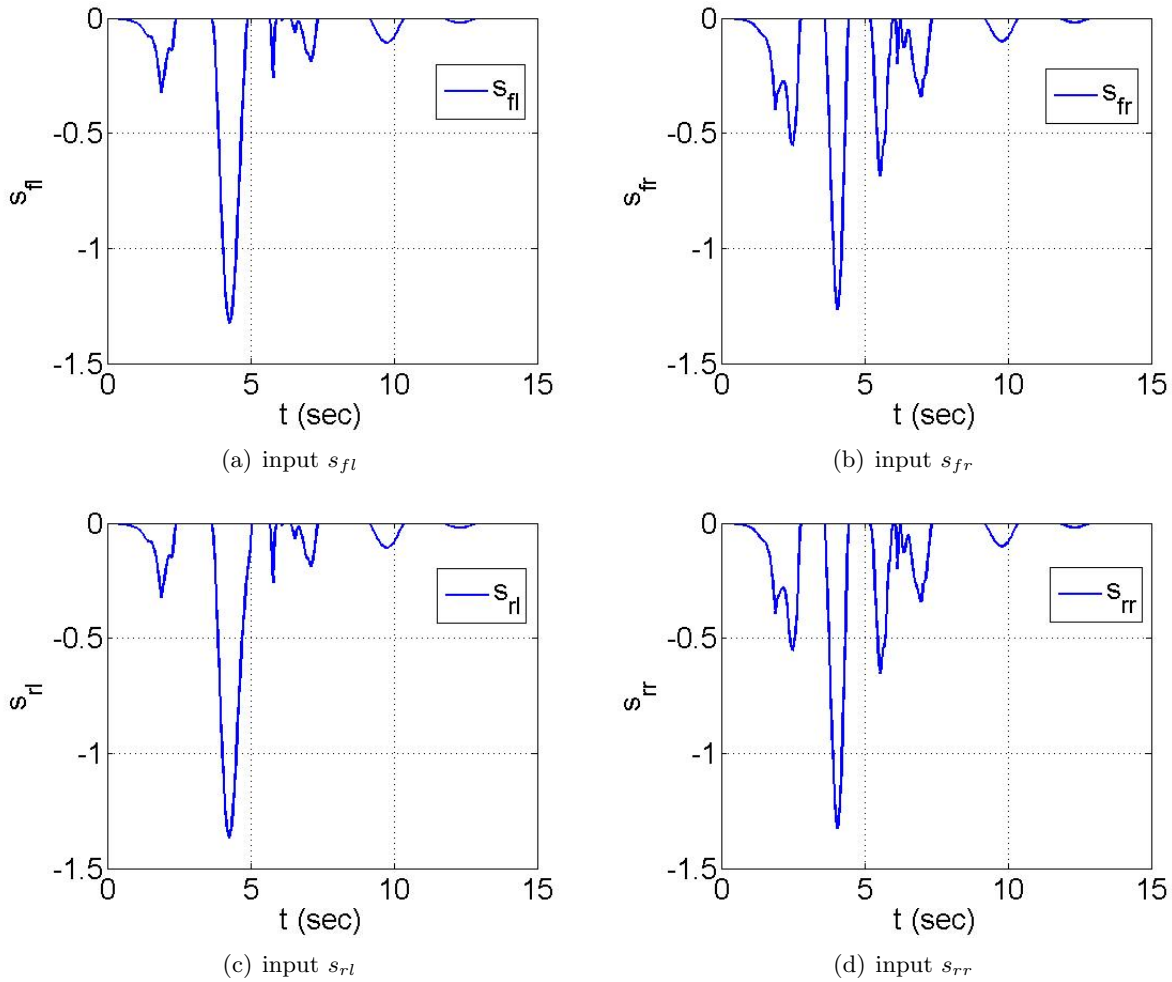

(a) input s_{fl} (b) input s_{fr}

(c) input s_{rl} (d) input s_{rr}

Figure 8: Slip ratios at four wheels with improved LTVMPC.

6(c). Also improved LTVMPC reaches steady state faster than that of LTVMPC which can be seen by comparing fig 6(b) and 6(d) with 3(b) and 3(d) respectively.

Fig 7 shows the steering angle and its increment for improved LTVMPC. Both of these values are within the constraints. By comparing input steering angle for LTVMPC shown in fig 4(a) with the input steering angle for improved LTVMPC in fig 7(a), it can be seen that input for LTVMPC reaches the boundary value of 10° and for improved LTVMPC this value is well within its bounds.

Fig 8 shows the slip ratio at four wheels with the improved LTVMPC. As with the LTVMPC here also the braking shown is differential braking where more brakes has been applied to right wheels so that vehicle will turn right. Comparison of fig 8 with fig 5 clearly shows that the braking applied with the improved controller is less than the braking with LTVMPC. This is in accordance with the velocity profiles in fig 3(a) and fig 6(a) where the effect of less braking as in fig 8 is reflected on the higher velocity being maintained in fig 6(a) in comparison to the velocity observed in fig 3(a).

The effect of the improved LTVMPC on its tracking performance will be directly reflected in the rms values of error. This is shown in table 1. In the table, ψ is in degree, $\dot{\psi}$ is in degree/sec and Y is in meter.

Table 1: Comparison of improved LTVMPC with LTVMPC

Controller		e_{avg}	e_{min}	e_{max}	e_{rms}
LTVMPC	ψ	1.0836	-3.6500	16.2548	4.6595
	$\dot{\psi}$	-1.7172	-21.3342	10.74186	5.9206
	Y	-0.3821	-3.5790	0.6580	0.9294
Improved LTVMPC	ψ	0.7907	-2.4357	13.0706	3.1355
	$\dot{\psi}$	-1.4964	-19.0279	4.1650	4.7914
	Y	-0.2862	-3.0738	0.2113	0.7114

From comparison it is seen that rms value of error is substantially less with the improved LTVMPC for all the 3 output variables; this reduction in error being 32.70%, 17.07% and 23.45% for ψ, $\dot{\psi}$ and Y respectively for the entry speed of $21m/sec$.

5. Conclusion

An improved linear time varying model predictive control (LTVMPC) for combined front wheel steering and four wheel braking of autonomous vehicle has been discussed. The performance of the controller for double lane change trajectory on low frictional road has been presented. The LTVMPC controller as reported earlier in literature has been modified by improvising on the linearization of the nonlinear model for the autonomous vehicle which is used for the design of steering control with braking. The accuracy in the linearization is directly reflected on the tracking performance with high entry speed during double lane change. Simulation results are presented to show the efficacy of the methodology. Comparison of the simulation results from LTVMPC and improved LTVMPC shows that the proposed methodology leads to better traits in tracking performance.

References

[1] Falcone P, Borrelli F, Asgari J, Tseng H E, and Hrovat D 2007 Predictive active steering control for autonomous vehicle systems, *IEEE Trans. Control System Technology.***15** 566-580.
[2] Borrelli F, Falcone P, Keviczky T, Asgari J, and Hrovat D 2005 MPC-based approach to active steering for autonomous vehicle systems *Int. J. Veh. Autonomous Syst.* **3** 265-291.
[3] Falcone P, Tufo M, Borrelli F, Asgari J and Tseng H E 2007 A linear time varying model predictive control approach to the integrated vehicle dynamics control problem in autonomous systems *Proc. of the 46th IEEE Conf. on Decision and Control (New Orleans)* 2980-2985.
[4] Falcone P, Borrelli F, Asgari J, Tseng H E, and Hrovat D 2007 A model predictive control approach for combined braking and steering in autonomous vehicles *15th Mediterranean Conf. on Control and Automation.*
[5] Mayne D, Rawlings J, Rao C and Scokaert P 2000 Constrained model predictive control: Stability and optimality *Automatica* **36** 789-814.
[6] Mayne D 2001 Control of constrained dynamic systems *European J. of Control* **7** 87-99.
[7] Bakker E, Nyborg L and Pacejka H B 1987 Tyre modeling for use in vehicle dynamics studies *SAE paper No. 870421.*
[8] Palmieri G, Barbarisi O, Scala S and Glielmo L 2010 On low complexity predictive approaches to control of autonomous vehicles *Springer book* 195-210.
[9] Kerrigan, Eric C and Jan M 2000 Soft constraints and exact penalty functions in model predictive control *Control Conf. (Cambridge).*
[10] Scokaert, Pierre O and James B 1999 Feasibility issues in linear model predictive control *AIChE J.* **45** 1649-1659.